ChemComm

COMMUNICATION

View Article Online
View Journal | View Issue

Cite this: *Chem. Commun.*, 2022, **58**, 3497

Received 20th December 2021,
Accepted 11th February 2022

DOI: 10.1039/d1cc07128a

rsc.li/chemcomm

Potassium *tert*-butoxide promoted regioselective deuteration of pyridines†

Yan Li,[ab] Chenxu Zheng,[ab] Zhi-Jiang Jiang,*[a] Jianbo Tang,[ac] Bencan Tang[d] and Zhanghua Gao*[a]

A regioselective deuteration at the β- and γ-position of pyridines is reported. Efficient deuteration occurred with a combination of KO^{t}Bu and DMSO-d_6, replenishing the prevailing α-deuteration of the pyridine systems. Preliminary mechanistic studies suggested that the dimsyl carbanion acts as one of the key intermediates.

Over the past few years, deuterium labelling has received substantial attention as a well-known tool for both biological metabolite investigation and reaction mechanism elucidation.[1] Benefiting from the prominent kinetic isotope effect, the enhanced C–D bond has shown promising applications in the pharmaceutical and material industries by controlling the metabolism of drugs, improving the stability of materials, and elevating the efficiency of photoelectric devices.[2] Thus, the diverse requirement of both deuterated scaffolds and regioselective deuterium-labelling is increasing, and the strengthening of the deuteration arsenal has been accelerated during recent years.[3]

Pyridines, as one of the prevailing N-heterocycles, have been employed in various chemical domains,[4] especially in the recent burgeoning fields including photocatalysis and photoelectric devices.[5] In pharmaceutical science, pyridines have also been identified as the second most common N-heterocycle,[6] and they have been employed as the core structure in a number of drugs. Current deuteration of pyridines has been primarily focused on hydrogen isotope exchange (HIE) at the α-position using Pd,[7] Rh,[8] Ir,[8a] Ru,[8c,9] and Ni[10] catalysts (Fig. 1A). In contrast, the HIE at other positions on pyridines has rarely

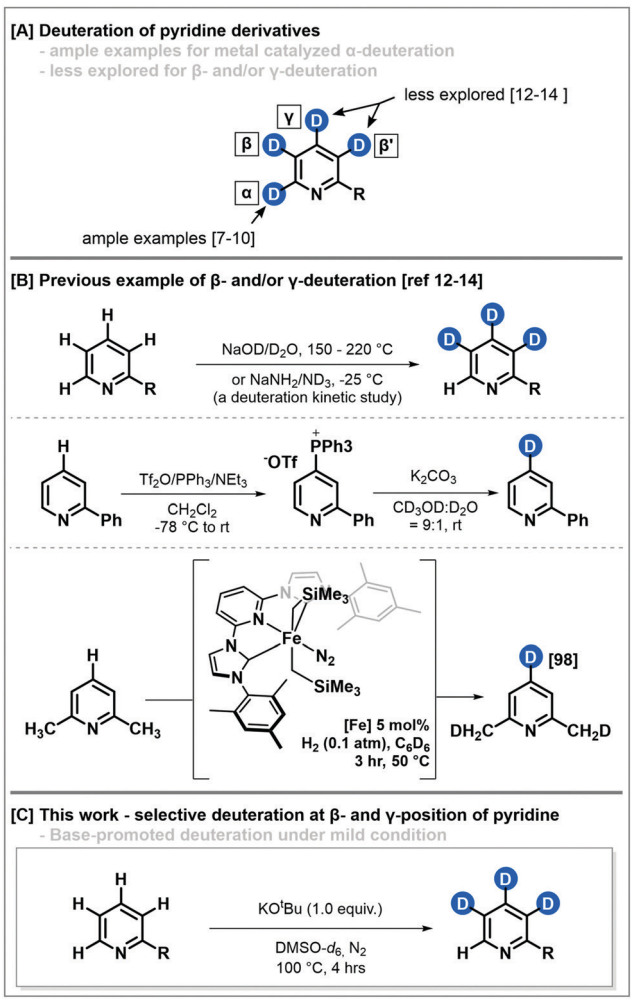

Fig. 1 (A) Site selective deuteration of pyridines. (B) Previous examples of deuteration at the β- and/or γ-positions of pyridines. (C) Regioselective deuteration at the β- and γ-positions of pyridines.

[a] *School of Biological and Chemical Engineering, NingboTech University, Ningbo, 315100, People's Republic of China. E-mail: zj.jiang@nbt.edu.cn, z.gao@nbt.edu.cn*
[b] *College of Chemical and Biological Engineering, Zhejiang University, Hangzhou, 310012, People's Republic of China*
[c] *College of Chemistry and Chemical Engineering, Lanzhou University, Lanzhou, 730000, People's Republic of China*
[d] *Department of Chemical and Environment Engineering, The University of Nottingham Ningbo China, Ningbo, 315100, People's Republic of China*

† Electronic supplementary information (ESI) available: Optimization and kinetic profile data, comparison spectra and characterization of the substrate and deuterated compounds. See DOI: 10.1039/d1cc07128a

been discussed. Apart from the deuteration by tautomerization of aminopyridines,[11] only a kinetic analysis half a century ago suggested a base-promoted deuteration under harsh conditions (Fig. 1B).[12] Recently, selective deuteration at the γ-position has been achieved by a phosphonium salt mediated defunctionalization deuteration.[13] Moreover, the Chirik group reported the γ-deuteration of 2,6-dimethylpyridnine *via* Fe-pincer catalyzed HIE, in which the regioselectivity was controlled by the steric hindrance.[14]

During our recent attempts at the synthesis of deuterated photoelectric materials, an unexpected deuteration ratio of over 500% was observed when preparing 5-trideuteromethyl-2-phenylpyridine (**2**) under basic conditions. We discovered that the β, γ, and β′ positions of the pyridine ring were deuterated nearly quantitatively, leaving the α-site nearly untouched. Herein, we present our preliminary results of this base-promoted deuteration of the β- and γ-positions of pyridines (Fig. 1C).

The initial optimization was conducted using 2-phenyl pyridine (**1**) as a model substrate to eliminate the influence of methyl deuteration (Fig. 1C, see the ESI† for the detailed optimization data). The experiments showed the combination of KO^{t}Bu and DMSO-d_6 to be the optimal condition for this pyridine HIE,[15] affording three position deuteration with 2.97D[16] with 1.0 equivalent of KO^{t}Bu.[17] A slight retardation of the HIE was observed with potassium hydroxide, which reached 2.02D and 2.52D after 4 and 18 hours, respectively. Other bases including NaO^{t}Bu and LiO^{t}Bu failed to render acceptable results. Shifting the deuterium source to D_2O, $CDCl_3$, or CD_3OD did not give any satisfactory results in this HIE process (see the ESI† for the optimization data).

We then studied the influence of the amount of KO^{t}Bu in this reaction. The sub-stoichiometric amounts of KO^{t}Bu, such as 0.5 and 0.1 equivalent, also rendered deuterium incorporation of 2.65D and 1.71D after 18 hours, respectively, which aroused our interest in the kinetic feature of this HIE process. Thus, the reaction was tracked using different KO^{t}Bu loadings (Fig. 2A, see the ESI† for the detailed data). Interestingly, the reactions with 1.0 to 2.5 equivalent of KO^{t}Bu provided similar deuterium accumulation, which reached 2.5D at the end of the first hour, suggesting that saturation was reached in terms of the kinetic behavior of KO^{t}Bu when 1.0 equivalent was used. Meanwhile, a much slower exchange was observed in sub-stoichiometric cases, which offered us an opportunity to determine the site-specific deuterium incorporation by NMR analysis (Fig. 2B). As expected, the high KO^{t}Bu-loading rendered an evenly high deuterium-incorporation at the β, γ, and β′-positions without discrimination. In contrast, priority was observed at the γ-position in both sub-stoichiometric cases. Noticeably, a neglectable deuteration could be observed at the α-position, and a similar degree of deuteration could also be detected at the *ortho*-position of the adjacent phenyl ring.

With these data in hand, the mechanism was questioned for this selective deuteration at the β- and γ-positions of the pyridines. The control experiments were carried out to gain an insight into the mechanism. As a representative system for the radical process, the combination of KO^{t}Bu/DMSO has shown synthetic applications in various transformations,

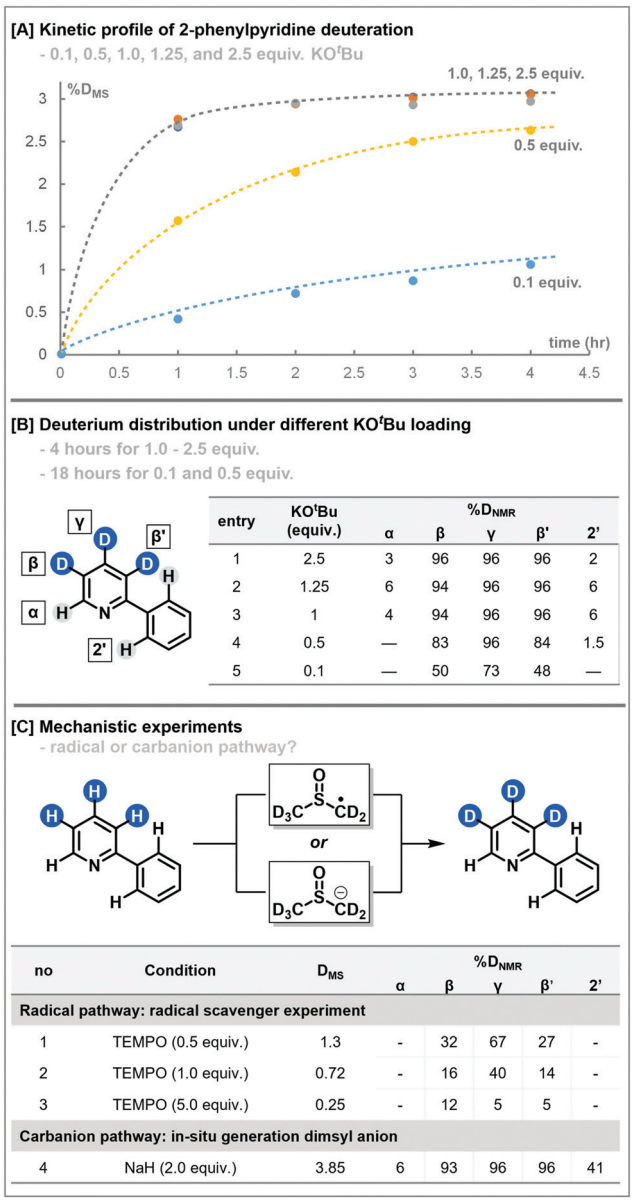

entry	KO^{t}Bu (equiv.)	%D$_{NMR}$ α	β	γ	β′	2′
1	2.5	3	96	96	96	2
2	1.25	6	94	96	96	6
3	1	4	94	96	96	6
4	0.5	—	83	96	84	1.5
5	0.1	—	50	73	48	—

no	Condition	D$_{MS}$	%D$_{NMR}$ α	β	γ	β′	2′
Radical pathway: radical scavenger experiment							
1	TEMPO (0.5 equiv.)	1.3	-	32	67	27	-
2	TEMPO (1.0 equiv.)	0.72	-	16	40	14	-
3	TEMPO (5.0 equiv.)	0.25	-	12	5	5	-
Carbanion pathway: in-situ generation dimsyl anion							
4	NaH (2.0 equiv.)	3.85	6	93	96	96	41

Fig. 2 (A) Kinetic profile of the deuteration procedure under different KO^{t}Bu loadings. (B) Deuterium distribution under different KO^{t}Bu loadings. (C) Mechanistic experiments. TEMPO = 2,2,6,6-tetramethylpiperidyl-1-oxyl.

including deuteration, cyclization, and methylation.[18] Thus, our first hypothesis presumed the reaction as a KO^{t}Bu/DMSO mediated radical process, and the radical scavenger, 2,2,6,6-tetramethyl piperidine 1-oxyl radical (TEMPO), was expected to suppress the HIE (Fig. 2C). Although a dramatic retardation was observed, the reaction was not completely suppressed even at more than 5.0 equivalents of TEMPO. Then, we turned our attention to verifying the possibility of the carbanion pathway,[19] which had been studied kinetically in protic environments by Zoltewicz and co-workers.[12a] This work suggested an acidic strength of 12 : 9.3 : 1.0 at the γ-, β-, and α-positions on the pyridines, respectively. Thus, the substrate was treated with the *in situ* prepared dimsyl anion. Although GC–MS showed a 3.85D incorporation, the following NMR analysis suggested

Table 1 Substrate scope[ab]

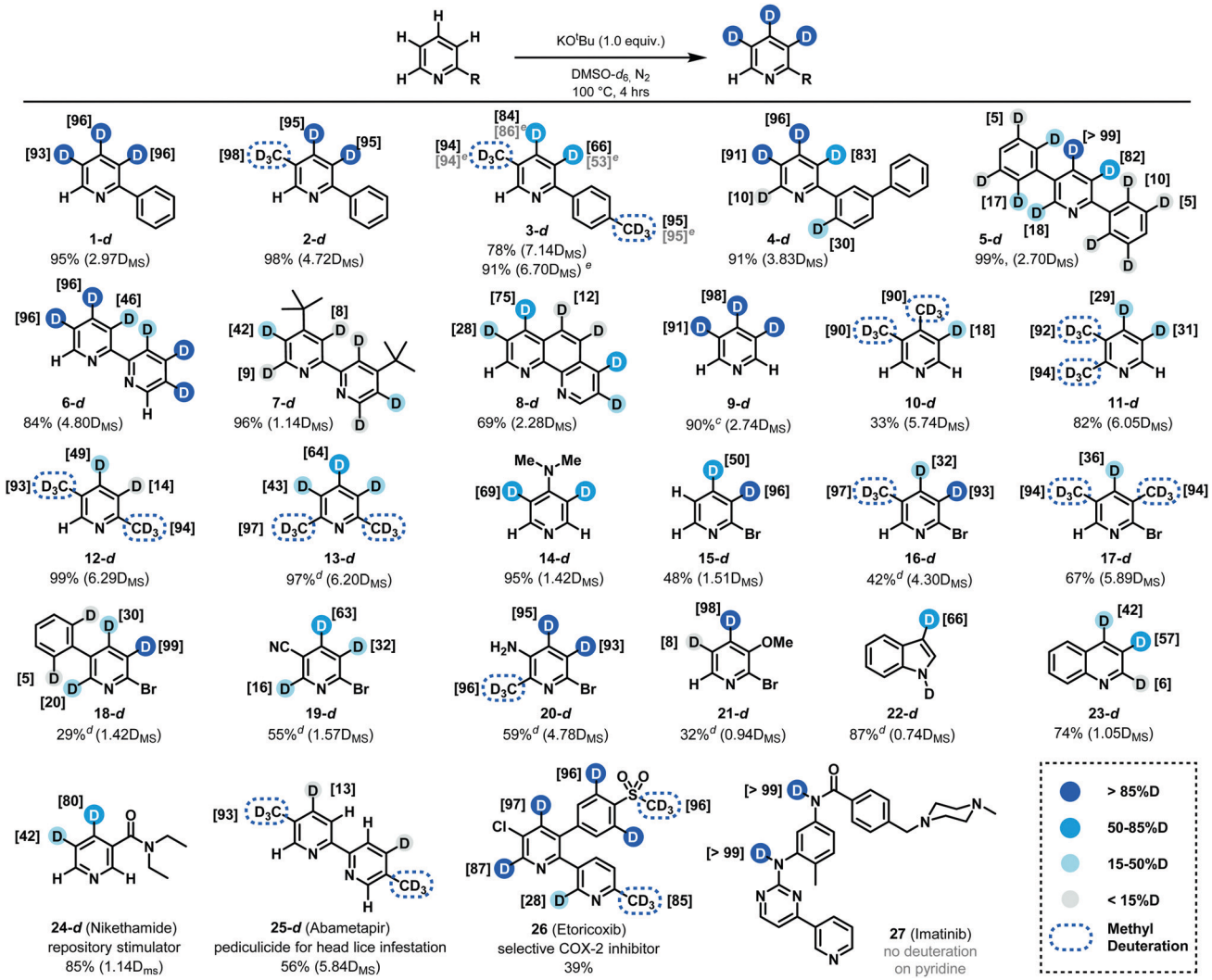

[a] Reaction conditions unless otherwise noted: pyridine derivatives (1.0 mmol), KO^{t}Bu (2.0 equiv.), and DMSO-d_6 (2 mL, approx. 23 equiv.) in a pressure vessel with N_2 protection, 100 °C, and 4 hours. [b] Deuterium incorporation determined by GC–MS (denoted in parentheses as %D$_{MS}$) and ^{1}H-NMR (denoted in square brackets at the specific site). Signal integral variation less than 5% was ignored in the substrate scope examination. [c] Yield calculated by GC analysis. [d] The yield and deuteration degree were investigated by ^{1}H-NMR with an internal standard. [e] Data of the gram-scale experiment of **3** (10 mmol, 1.89 g).

that the additional 0.85 position was distributed mainly at the 2′-site on the phenyl ring. However, the key α-position remained at a low-degree of deuterium incorporation. Thus, the current evidence supported the carbanion pathway as a main route for this KO^{t}Bu-mediated pyridine HIE, but a radical mechanism may also contribute simultaneously. In addition, the deprotonation at the α-position will generate an increased electron density in both cases, which raises an electronic repulsion with the lone-pair of nitrogen, and finally leads to the regioselectivity at the β- and γ-positions.[12a]

Subsequently, the substrate scope of this pyridine HIE was examined (Table 1). In the initial test set of 2-aryl pyridines (**1**–**8**), the γ-site possessed the maximal deuterium abundance as expected. The substrate with methyl substitution led to a slightly lower efficiency on pyridine deuteration (**2** and **3**). In some cases (*e.g.* **4**, **5**, **7**,**18** and **23**), deuterium was detected at the α-position, which may be caused by the expanded aromatic system. A similar phenomenon has also been observed on the adjacent phenyl rings. The 2′-deuterium level on the phenyl substituents increased in 2-(3′-biphenyl)pyridine (**4**) to 30%, and in 2,5-diphenyl pyridine (**5**) to 17% and 10% for the 2-positions in the two benzyl rings in **5**, respectively. Furthermore, a slight *meta*-deuteration was observed for the large polyaromatic system in **5**. When replacing the phenyl ring with a pyridyl ring (**6**), the deuterium level at the β and γ-positions remained at an excellent degree, with a significant decrease in β′-deuteration and an elevation in α-deuteration observed. The introduction of *tert*-butyl (**7**) led to a suppression of the overall deuteration. And 1,10-phenanthroline (**8**) gave similarly low deuteration on the alkene bridge motif.

Then, we shifted our focus to simple pyridine derivatives (**9–21**). Pyridine (**9**) afforded a standard result, where the β- and γ-positions rendered considerable deuterium abundance. The overall deuteration was still located at the β-, γ-, and β′-positions with methyl substituted pyridines (**10–13**). Noticeably, an unusual decrease in deuteration on the pyridines was observed in these cases again, especially with 2, 6-dimethyl pyridine (**13**). This phenomenon showed the important nature of the HIE as an equilibration process: the deuterated product could participate in the exchange continuously, where more acid protons occupied the HIE reaction opportunity, retarding the exchange of lower ones.

In contrast, the deuterium distribution changed when placing a mild electro-withdrawing substituent on the pyridine. Using 2-bromopyridine as the substrate, the deuterium accumulated followed by the inductive effect from bromine (**15–18**). The speculation was further supported by 2-bromo-5-cyanopyridine (**19**), where the cyano group overrode the induction of bromine. The electro-donating groups' facilitation of *ortho*-deuteration was observed again in the deuteration of **14**, **20**, and **21**, which had been noted in our previous work.[20]

Finally, the conditions were tested for heterocycles and sophisticated structures. Indole (**22**) showed a moderate level of deuterium accumulation at the C-3 position. Quinoline (**23**) also rendered a different deuteration pattern from the cases of pyridines, with deuterium levels of 42%, 57%, and 6% at the γ-, β-, and α-positions, respectively. Nikethamide (**24**), a repository stimulator bearing an amide side chain, was also tolerated under the standard conditions, affording 80% and 42% deuterium at the β- and γ-position, respectively. Abametapir (**25**), a pediculicide for head lice infestation, showed a much lower deuterium incorporation of 13% at the γ-position. The deuteration of etoricoxib **26** was achieved with an interesting deuterium distribution, especially at the *ortho*-sites of the sulfonyl. However, no expected deuteration was observed with imatinib **27**, which may be shaded by the rapid H/D exchange of active protons.

In summary, a KO^{t}Bu-promoted β- and γ-regioselective hydrogen-isotope exchange for pyridines has been developed by using DMSO-d_6 as the deuterium source, leaving the α-position nearly intact. Control experiments suggested a carbanion mechanism as one of the main pathways for the exchange. The protocol complements the prevailing methods for metal-catalysed α-deuteration of pyridines and is expected to find applications in photoelectric materials and biologically active molecules.

This work was supported by the Ningbo Natural Science Foundation (Grant No. 202003N4310) and the Ningbo Science and Technology Bureau under CM2025 Programme (Grant No. 2020Z092). We acknowledge Ningbo CYC chemicals for NMR analysis and deuterated reagent support. J. Z. J. thanks the Start-up Foundation from NingboTech University (No. 20191114).

Conflicts of interest

There are no conflicts of interest to declare.

Notes and references

1 (*a*) K. B. Wiberg, *Chem. Rev.*, 1955, **55**, 713–743; (*b*) E. M. Simmons and J. F. Hartwig, *Angew. Chem., Int. Ed.*, 2012, **51**, 3066–3072; (*c*) I. Polvoy, H. Qin, R. R. Flavell, J. Gordon, P. Viswanath, R. Sriram, M. A. Ohliger and D. M. Wilson, *Metabolites*, 2021, **11**, 570.
2 (*a*) T. G. Gant, *J. Med. Chem.*, 2014, **57**, 3595–3611; (*b*) H. Tsuji, C. Mitsui and E. Nakamura, *Chem. Commun.*, 2014, **50**, 14870–14872; (*c*) C. C. Tong and K. C. Hwang, *J. Phys. Chem. C*, 2007, **111**, 3490–3494; (*d*) X. Ma, Y. Wang, Y. Fan, F. Bai and J. Xu, *Chem. Res. Chin. Univ.*, 2018, **34**, 781–785.
3 (*a*) J. Atzrodt, V. Derdau, W. J. Kerr and M. Reid, *Angew. Chem., Int. Ed.*, 2018, **57**, 1758–1784; (*b*) J. Atzrodt, V. Derdau, W. J. Kerr and M. Reid, *Angew. Chem., Int. Ed.*, 2018, **57**, 3022–3047; (*c*) W. J. Kerr, G. J. Knox and L. C. Paterson, *J. Labelled Compd. Radiopharm.*, 2020, **63**, 281–295; (*d*) R. Zhou, L. Ma, X. Yang and J. Cao, *Org. Chem. Front.*, 2021, **8**, 426–444.
4 C. Allais, J.-M. Grassot, J. Rodriguez and T. Constantieux, *Chem. Rev.*, 2014, **114**, 10829–10868.
5 (*a*) S. Gisbertz, S. Reischauer and B. Pieber, *Nat. Catal.*, 2020, **3**, 611–620; (*b*) J. Ma, Y. Zhai, J. Chen, X. Zhou, W. Shi, J. Zhang, G. Li and H. Hou, *Tetrahedron*, 2020, **76**, 131054; (*c*) B. Baptayev, S. H. Lee, D. H. Kim and M. P. Balanay, *Chem. Phys. Lett.*, 2019, **730**, 407–410; (*d*) R. Chen, L. Wang, Z. An, X. Chen and P. Chen, *Liq. Cryst.*, 2021, **48**, 2178–2187.
6 (*a*) M. Baumann and I. R. Baxendale, *Beilstein J. Org. Chem.*, 2013, **9**, 2265–2319; (*b*) E. Vitaku, D. T. Smith and J. T. Njardarson, *J. Med. Chem.*, 2014, **57**, 10257–10274.
7 K. A. Guy and J. R. Shapley, *Organometallics*, 2009, **28**, 4020–4027.
8 (*a*) S. C. Schou, *J. Labelled Compd. Radiopharm.*, 2009, **52**, 376–381; (*b*) S. Chen, G. Song and X. Li, *Tetrahedron Lett.*, 2008, **49**, 6929–6932; (*c*) E. Alexakis, J. R. Jones and W. J. S. Lockley, *Tetrahedron Lett.*, 2006, **47**, 5025–5028.
9 (*a*) B. Gröll, M. Schnürch and M. D. Mihovilovic, *J. Org. Chem.*, 2012, **77**, 4432–4437; (*b*) G. Pieters, C. Taglang, E. Bonnefille, T. Gutmann, C. Puente, J.-C. Berthet, C. Dugave, B. Chaudret and B. Rousseau, *Angew. Chem., Int. Ed.*, 2014, **53**, 230–234.
10 H. Yang, C. Zarate, W. N. Palmer, N. Rivera, D. Hesk and P. J. Chirik, *ACS Catal.*, 2018, **8**, 10210–10218.
11 (*a*) N. Kebede and J. W. Pavlik, *J. Heterocycl. Chem.*, 1997, **34**, 685–686; (*b*) A. Y. Vorob'ev, V. I. Supranovich, G. I. Borodkin and V. G. Shubin, *Beilstein J. Org. Chem.*, 2017, **13**, 800–805.
12 (*a*) J. A. Zoltewicz, G. Grahe and C. L. Smith, *J. Am. Chem. Soc.*, 1969, **91**, 5501–5505; (*b*) J. A. Zoltewicz and J. D. Meyer, *Tetrahedron Lett.*, 1968, **9**, 421–426.
13 J. L. Koniarczyk, D. Hesk, A. Overgard, I. W. Davies and A. McNally, *J. Am. Chem. Soc.*, 2018, **140**, 1990–1993.
14 J. Corpas, P. Viereck and P. J. Chirik, *ACS Catal.*, 2020, **10**, 8640–8647.
15 Phenylpyridine **1** (1.0 mmol), KO^{t}Bu (2.0 equiv.), DMSO-d_6 (2 mL) in a pressure vessel with N_2 protection, 100 °C, 4 hours.
16 2.97D represented for an average deuterium-incorporation in one molecule is 2.97, which was calculated by GC–MS. For calculation method, see our previous publication: ref. 20.
17 The theoretical deuterium ratio for three deuterated sites in this reaction is approx. 98% for one position, and the overall theoretical deuterium incorporation should be 2.96D.
18 (*a*) Y. Hu, L. Liang, W.-T. Wei, X. Sun, X.-J. Zhang and M. Yan, *Tetrahedron*, 2015, **71**, 1425–1430; (*b*) Y.-Y. Chen, J.-H. Chen, N.-N. Zhang, L.-M. Ye, X.-J. Zhang and M. Yan, *Tetrahedron Lett.*, 2015, **56**, 478–481; (*c*) L. Pan, M. V. Cooke, A. Spencer and S. Laulhé, *Adv. Synth. Catal.*, 2022, **364**, 420–425; (*d*) S. Jiang, Z. Yang, Z. Guo, Y. Li, L. Chen, Z. Zhu and X. Chen, *Org. Biomol. Chem.*, 2019, **17**, 7416–7424.
19 M. Patel, R. K. Saunthwal and A. K. Verma, *ACS Omega*, 2018, **3**, 10612–10623.
20 J. Kong, Z.-J. Jiang, J. Xu, Y. Li, H. Cao, Y. Ding, B. Tang, J. Chen and Z. Gao, *J. Org. Chem.*, 2021, **86**, 13350–13359.

